Journal of Solid State Chemistry **146,** 39–46 (1999)
Article ID jssc.1999.8302, available online at http://www.idealibrary.com on IDEAL®

Formation of α,β-Type Hydroxides and Second-Stage Intermediate in Hydrothermal Decomposition of Nickel Acetate

H. Nishizawa,[1] T. Kishikawa, and H. Minami

Department of Chemistry, Faculty of Science, Kochi University, Kochi 780, Japan

Received December 24, 1998; in revised form March 16, 1999; accepted March 23, 1999

During heating of nickel acetate solution at a constant rate of 4°C/min up to 350°C, α-type anion-exchangeable layered hydroxide $Ni_2(OH)_3(OCOCH_3)1.4H_2O$, containing the acetate anions in the interlayer spaces, first crystallized at 160°C. A second-stage intermediate phase losing the acetate guest in every second layer appeared at 180°C and subsequently transformed at 210°C to slightly disordered β-$Ni(OH)_2$ phase with a small amount of acetate anions. β-$Ni(OH)_2$ phases were gradually losing the acetate guest with increasing temperature, and perfectly ordered hexagonal-shaped β-$Ni(OH)_2$ crystals with a mean diameter of 10 μm were obtained at 320°C. Above 340°C, dehydration of β-$Ni(OH)_2$ to NiO occurred. © 1999 Academic Press

INTRODUCTION

The increasing demand for higher quality inorganic oxides for electronic, ceramic, and pigment applications has prompted industry to search for alternate processes to produce these materials. The hydrothermal decomposition and crystallization method has a greater prospect of producing higher quality inorganic oxide powders (1–3) and thin films (4–8).

This method possesses several advantages: the oxide powders and the thin films of various inorganic compounds, including hydroxides and hydrates, may be prepared at a relatively low temperature and for a short time.

The powders and the films of anion-exchangeable layered mixed basic salt, $Ni_{1-x}Zn_{2x}(OCOCH_3)_2xH_2O$ (LMBA), have been recently synthesized through the hydrothermal decomposition of a mixed aqueous solution of zinc and nickel acetates (8). LMBA crystallized at 130°C from Zn–Ni mixed acetate solutions with Zn/Ni molar ratios from 0.2 to 10. The LMBA thin film obtained at 130°C in Zn-rich solutions showed *c* axis orientation perpendicular to the substrate surface.

Zinc acetate was found to be hydrothermally decomposed above 120°C, resulting in the formation of polycrystalline ZnO. The hexagonal columnar ZnO crystals with a mean diameter of 2 μm were obtained by hydrothermal treatment of 0.3 M zinc acetate solution at 120°C for 1 h (7). On the other hand, the hydrothermal treatment of nickel acetate resulted in the formation of new basic nickel acetates with a layered structure of basal spacing, 0.944 and 1.415 nm, as the precursor phases of nickel hydroxide. Especially the 1.415 nm phase was very unstable and easily transformed to nickel hydroxide.

Many studies have been devoted to nickel hydroxide because most secondary alkaline cells contain nickel hydroxide-positive electrodes at which reversible oxidation to nickel(III) or even nickel(IV) oxide hydroxides occurs. There are two structural types for nickel hydroxides. β-$Ni(OH)_2$ is isomorphous with brucite and crystallizes in the hexagonal system while α-$Ni(OH)_2$ has a disordered lamellar structure. For β-$Ni(OH)_2$, the definite structure determination has been made by Greaves and Thomas (9) with powder neutron diffraction. In most cases, the active material of positive electrodes belongs to the β structural type with very small crystalline sizes with probable structural defects. So far, α-type nickel hydroxides are not extensively used in commercial cells, though such active materials show good electrochemical performances. This is because the α-type nickel hydroxides are unstable in alkaline or aqueous media and are converted within a few hours into the β structural type through a dissolution–recrystallization reaction (10). It is very interesting to investigate the crystallization process of β-$Ni(OH)_2$ under hydrothermal conditions.

In the present work, the process of the formation of β-$Ni(OH)_2$ from nickel acetate under hydrothermal conditions was examined by the use of a constant-rate heating and rapid quenching method (11–12). The phases formed during decomposition of nickel acetate were characterized by X-ray diffraction (XRD), Fourier transform–infrared spectra (FT–IR), thermogravimetric–differential thermogravimetric (TG–DTA), and chemical analyses.

[1] To whom correspondence should be addressed.

0022-4596/99 $30.00

EXPERIMENTAL DETAILS

1. Hydrothermal Reaction

Hydrothermal experiments were conducted by heating 5 ml of nickel acetate aqueous solution in a microautoclave. To prepare the starting solutions, the $Ni(CH_3COO)_2 4H_2O$ (guaranteed reagent grade, Wako Pure Chemical Industry, Ltd., Osaka, Japan) was dissolved in redistilled water at a concentration of 0.5 M (mol/dm^3). The solution was inserted directly into a microautoclave (lined with Hasteloy-C) with a capacity of 8 cm^3 that was used as a reaction vessel. The vessel was heated by means of a well-insulated tabular furnace; the heating rate was controlled at 4°C/min from 50 to 350°C. The reaction temperatures are about 10°C higher than the actual values in the vessel because they are measured at the outer wall of the microautoclave, but they are useful as a baseline for comparing the data. The reaction pressure gradually increased with increasing temperature as 5 ml of solution was sealed in the reaction vessel. The pressure increased in almost the same manner for all runs using 5 ml of solution, 6 and 16 MPa at 250 and 350°C, respectively. After the desired temperature was reached, the vessel was quenched rapidly to room temperature by immersing it in iced water. The powder products in the reaction vessel were completely recovered. They were filtered off and washed several times with distilled water, followed by drying in a desiccator at room temperature.

2. Characterization

The powder products were subjected to structural analysis using Rigaku X-ray diffraction equipment (Model RAD-II-C). FT–IR spectra were recorded using a JASCO FT/IR-5300 spectrometer for products dispersed in KBr pellets. The differential thermal, thermogravimetric, and differential thermogravimetric analyses (DTA–TGA–DTG) were carried out using MAC TG–DTA 2000 instrument for a heating rate of 10°C/min in air. The TEM study was carried out with a HITACHI H-800 transmission electron microscope. The nickel content was determined by atomic absorption spectrometry after dissolving the products in concentrated nitric acid. C and H were determined by CHN microanalysis.

3. Chemical Reaction

Chemical reactions with some organic compounds were conducted by immersing the powder samples in 0.5 M aqueous solutions of sodium octyl carboxylate ($Na^+CH_3(CH_2)_6COO^-$) (concentration about 0.5 M) or in *n*-propylamine ($C_3H_7NH_2$) solution and allowing them to react for up to 3 days at room temperature. The samples were occasionally shaken during these periods. The powder samples were washed with distilled water and centrifuged, followed by drying in a desiccator at room temperature. The products were characterized in a manner similar to the original ones.

RESULTS AND DISCUSSION

1. Hydrothermal Decomposition of Nickel Acetate

X-ray powder diffraction. Figure 1 shows XRD patterns of the samples obtained during heating of nickel acetate solution at a constant rate of 4°C/min. The very small amount of the pale-green powder sample was first obtained at 150°C. The XRD pattern of this powder sample shows well-defined peaks at 0.944, 0.4687, 0.2687, and 0.1554 nm

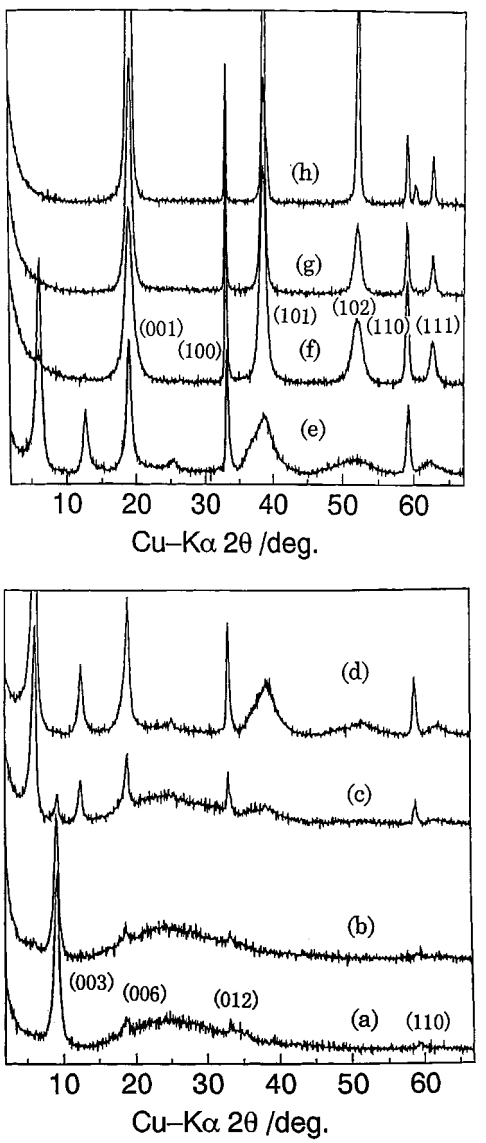

FIG. 1. XRD patterns of the samples obtained at (a) 160°C, (b) 170°C, (c) 180°C, (d) 190°C, (e) 200°C, (f) 210°C, (g) 230°C, and (h) 320°C, during heating of nickel acetate solution.

(Fig. 1a), which correspond, respectively, to the (003), (006), (101), and (110) reflections of α-$Ni(OH)_2$. α-$Ni(OH)_2$ obtained under hydrothermal conditions showed relatively good crystallinity, compared with those obtained by precipitation procedures (13–17).

The layered spacing of 0.944 nm changed little up to 170°C. A new crystalline phase with d spacing of 1.415 nm suddenly appeared with small residual phase ($d = 0.977$ nm) at 180°C which completely disappeared at 190°C. The XRD patterns of the powder samples obtained at 190 and 200°C showed similarities in the $15° \leq 2\theta \leq 70°$ range with that of β-type $Ni(OH)_2$ which appeared at above 210°C. But the distances corresponding to all peaks except for two peaks, $d = 0.2696$ and 0.1559 nm, are almost submultiple of one another, so that those peaks may belong to basal reflections. Two peaks below 15° completely disappeared at 210°C. β-$Ni(OH)_2$ with hexagonal lattice constants, $\alpha = 0.3126$ nm and $c = 0.4605$ nm, formed at 210°C as a single phase and crystal growth exceeded. The line widths of (101), (102), and (111) peaks of β-$Ni(OH)_2$ were gradually decreased with temperature up to 300°C. This means the ordering of the layer structure of β-$Ni(OH)_2$. Dehydration reaction from $Ni(OH)_2$ to NiO occurred at above 340°C.

Infrared spectra. Figure 2 shows the infrared spectra of the samples obtained during constant-rate heating and

TABLE 1
FT–IR Spectra Data[a] of Samples Obtained during Hydrothermal Decomposition of Nickel Acetate

Temperature (°C)								
160	170	180	190	200	210	230	280	320
		3646sh[b]	3646sh	3644sh	3644sh	3644sh	3642sh	3644sh
3538br	3538br	3569br	3567br					
				3424br	3424br	3447br	3445br	
3416br	3416br	3426br	3420br					
1593s	1593s	1607s	1611m	1624m	1613m	1624w	1635w	
1429s	1429s	1433s	1433m	1431m	1431m	1420w	1420w	
1385s	1385s	1381s	1379m	1379m	1381m	1381w	1379w	
1327s	1329s	1321s	1321m	1319m	1321m	1321w	1315w	
12020m	1020m	1019m	1019w	1019w	1017w	1017w		
656s	656s	654s	654s	652w				
		519s	519s	515s	515s	511s	509s	509s
476w	476w	467w	467w	469w	463w	467w	467w	

[a] Frequencies, ν, in cm^{-1}.
[b] sh, sharp; br, broad; s, strong; m, medium; w weak.

Table 1 provides wavenumber data of their peaks. In all these spectra, vibrations due to acetate group are seen in the 1700–1000 cm^{-1} region but intensities decrease with increasing temperature.

The IR spectra of α-$Ni(OH)_2$ obtained at 160 and 170°C show the intense bands at 1593 and 1385 cm^{-1}, assigned to

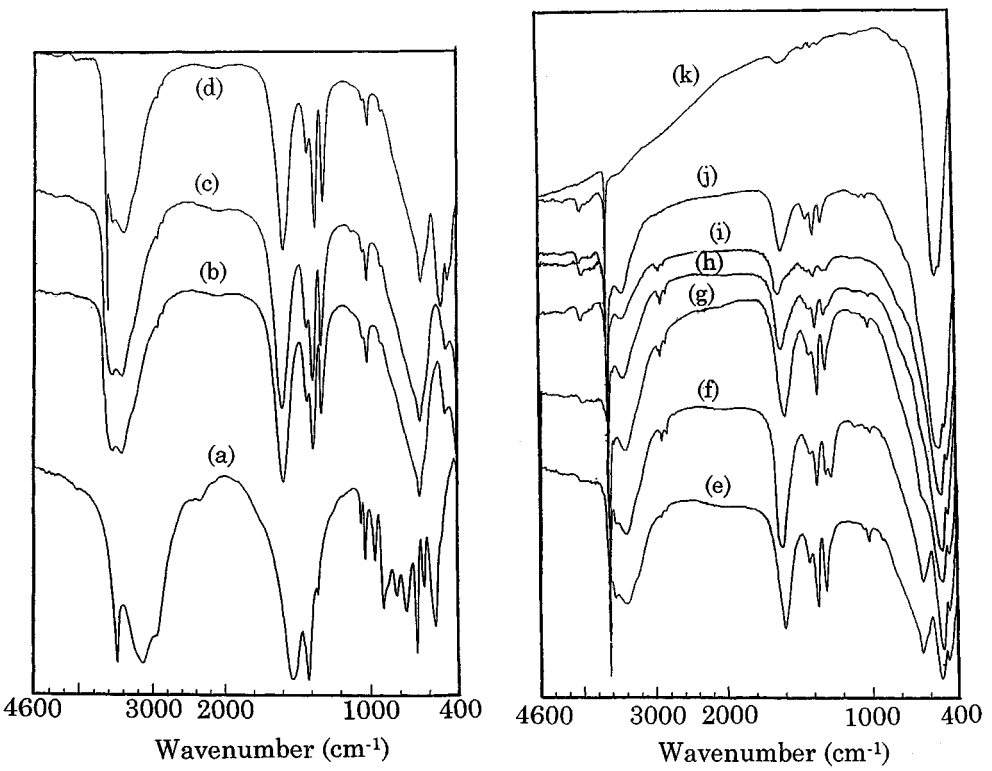

FIG. 2. FT–IR spectra of (a) nickel acetate and the samples obtained at (b) 160°C, (c) 170°C, (d) 180°C, (e) 190°C, (f) 200°C, (g) 210°C, (h) 230°C, (i) 250°C, (j) 280°C, and (k) 320°C during heating of nickel acetate solution.

ν_{as} (–COO^-) and ν_s (–COO^-), respectively (see Fig. 2a). The difference (208 cm^{-1}) between these two frequencies is characteristic of a unidentate acetate ligand (18). The proposed structural model contains the acetate fragment bound to the nickel atoms via a single oxygen atom. The intense bands at 3538, 3416, and 656 cm^{-1} are assigned to interlayer water or a hydroxyl group. The two slightly broad bands with strong intensity above 3400 cm^{-1} are assigned to stretching vibration of hydroxyl groups with weakly interacting hydroxyls and/or interlayer water. The hydroxyl bending band at 650 cm^{-1} (δOH) indicates that the hydroxyl groups of $Ni(OH)_2$ sheets are linked by hydrogen bonds to water molecules.

The IR spectra of α-$Ni(OH)_2$ prepared by adding ammonia solution to a nickel acetate solution that contained acetate ions as adsorbed species showed two bands of 1570 and 1390 cm^{-1}, which correspond to ν_{as} (–COO^-) and ν_s (–COO^-), respectively (19). Such a difference of two bands seems to correspond to the free acetate ions. This may be related to the lower crystallinity of α-$Ni(OH)_2$ prepared by the direct precipitation method.

In the spectra of β-$Ni(OH)_2$ obtained above 210°C, the bands characteristic of acetate groups were very weak and the difference (230 to 260 cm^{-1}) between ν_{as} (–COO^-) and ν_s (–COO^-) was slightly larger than that of α-$Ni(OH)_2$. Such a large difference in wavenumber suggests a loss of hydrogen bonds between the acetate and the water molecule in β-$Ni(OH)_2$. The sharp band at 3644 cm^{-1} is assigned to stretching vibration of OH groups not involved in hydrogen bonding, whereas broader bands at 3424–3447 cm^{-1} with medium intensity are assigned to weakly interacting hydroxyls and/or interlayer water.

In the intermediate phase obtained at 190°C, the spectra seemed to overlap α and β-$Ni(OH)_2$ spectra. The spectra showed the sharp band at 3646 cm^{-1} due to the stretching vibration of OH groups not involved in hydrogen bonding and also two slightly broad bands at 3567 and 3420 cm^{-1} due to hydrogen bonding OH, characteristic of α- and β-$Ni(OH)_2$, respectively. The bands due to acetate groups were seen in the 1700–1000 cm^{-1} region with relatively weak intensity. The two or three bands below 700 cm^{-1} may be assigned to Ni–O stretching vibrations. While the band at about 470 cm^{-1} appeared in all samples, the bands at about 650 and 510 cm^{-1} were characteristic of α-$Ni(OH)_2$ and β-$Ni(OH)_2$, respectively.

Thermal analysis. Figure 3 shows TG–DTA–DTG curves of the samples obtained at 160, 190, and 230°C. The DTA curve (Fig. 3a) of α-$Ni(OH)_2$ obtained at 160°C showed that the endothermic peak at 120°C corresponds to the loss of water molecules when the interlayer region first appeared. The second endothermic and subsequent exothermal peaks at 320–400°C seemed to be due to dissociation and combustion of hydroxyl and acetate groups, respectively. The DTG curve also showed weight losses in two stages. The composition of α-$Ni(OH)_2$ obtained at 160°C was determined to be $Ni_2(OH)_3(OCOCH_3)1.4H_2O$ by elemental analysis and TG results.

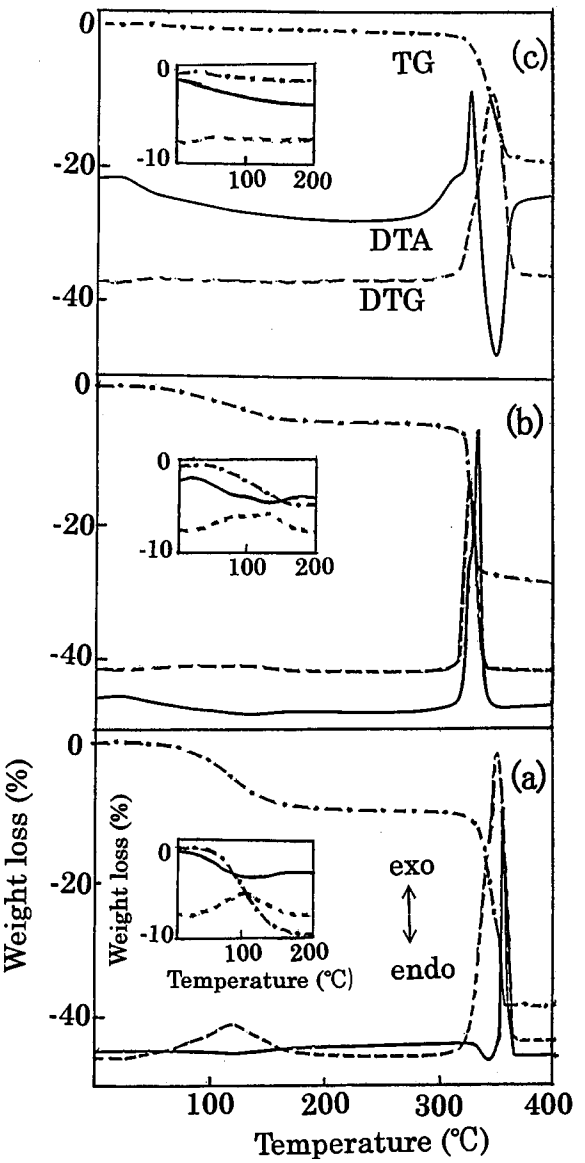

FIG. 3. TG–DTA–DTG curves (TG, dashed and dotted lines; DTA, solid lines; DTG, dashed lines) of the samples obtained at (a) 160°C, (b) 190°C, and (c) 230°C during heating of nickel acetate solution. The insets show the enlarged DTA curves with TG–DTG from room temperature to 200°C.

The DTA curve (Fig. 3c) of β-$Ni(OH)_2$ obtained at 230°C showed that the first peak at about 300°C due to dehydration almost disappeared and only the endothermic peak due to dissociation of hydroxyl groups appeared. The DTG curve showed a discernible shoulder on the lower temperature side that might be due to combustion of slight residual

acetate groups. This agreed with the exothermic peak of the DTA curve at 298°C. This slight exothermic peak became weak in intensity and was shifted to the higher temperature side by increasing the hydrothermal synthetic temperature (210–320°C). This agreed with the decrease in the content of acetate groups in β-$Ni(OH)_2$ estimated by FT–IR data.

The DTA–TG curve (Fig. 3b) of the intermediate phase obtained at 190°C showed the endothermic peak at 120°C due to dehydration and the exothermic peak at 320°C with a shoulder on the lower temperature side that may be due to the simultaneous occurrence of dissociation and combustion of hydroxyl and acetate groups, respectively. This is supported by the fact that the weight loss occurs in one step, shown in the TG–DTG curves. The composition of the intermediate phase was determined to be $Ni_2(OH)_{3.5}(OCOCH_3)_{0.5}0.5H_2O$ by elemental analysis and TG results.

Transmission electron microscopy. Transmission electron micrographs for selected samples are shown in Fig. 4. For α-$Ni(OH)_2$ obtained at 170°C, crystallites of thin plates showed square shapes with a mean diameter of 1 μm. Above 200°C, crystallites were broken up into several fragments and gradually lost their square shape with increasing temperature. The grain growth of β-$Ni(OH)_2$ occurred at above 250°C and hexagonal-shaped β-$Ni(OH)_2$ crystals with a mean diameter of 10 μm were formed at 320°C. At 340°C, NiO crystals formed by dehydration of β-$Ni(OH)_2$ retain the habit of the starting hydroxide but had a smaller crystalline size of about 1 μm.

2. Chemical Reactivity

The intercalation of a neutral species and the ion exchanging of alkyl-carboxylate anion were conducted to compare the chemical reactivity of the products obtained during hydrothermal treatment of nickel acetate solution. These reactions for β-$Ni(OH)_2$ resulted in only the recovery of the starting material. Figure 5 shows the changes in XRD patterns by the reaction of α-$Ni(OH)_2$ and the intermediate phase, obtained at 160 and 200°C, respectively, with *n*-propylamine solution. These showed systematic shift of the basal diffraction peaks for both phases toward low angles, indicating that an intercalation process had occurred. The increase in basal spacing of α-$Ni(OH)_2$ was 0.179 nm and nearly equal to that (0.140 nm) of the intermediate phase. It is noteworthy that the peak ($d = 0.4657$ nm) nearly coincident with the (001) diffraction peak of β-$Ni(OH)_2$ is also systematically shifted to a lower angle and there is no residual peak for β-$Ni(OH)_2$. This suggests that the intermediate phase is a single phase and not only contains α-$Ni(OH)_2$ and also β-$Ni(OH)_2$.

Figure 6 shows the changes in the interlayer distances by the alkyl-carboxylate exchanging of α-$Ni(OH)_2$ and the intermediate phase, obtained at 160 and 200°C, respectively, as a function of the number of carbon atoms in the alkyl chain. For α-$Ni(OH)_2$, the increment of the interlayer distance for each additional carbon atom is 0.23 nm/carbon atom, indicating the presence of a bilayer of alkyl chain in the interlayer region. For the alkyl-carboxylate-exchanged intermediate phases, an almost constant interlayer distance of 1.58 nm was observed. The interlayer distance was not dependent on the length of the alkyl chain. This may be attributed to the arrangement of the alkyl chains parallel to the layers. Kamath and Therese recently reported the possibility of anion exchanging by α-$Ni(OH)_2$ (20). α-$Ni(OH)_2$ has a hydrotalcite-like phase, possessing a layered double-hydroxide (LDH) structure even though there are no trivalent cations in the lattice. While the LDHs acquire a positive charge on the hydroxide layers by the incorporation of trivalent cations, α-hydroxyl ions acquire a positive charge by partial protonation of the hydroxyl ions according to the equation

$$M(OH)_2 + xH^+ \rightarrow [M(OH)_{2-x}(H_2O)_x]^{x+}.$$

As in the LDHs, charge balance is restored by the incorporation of anions in the interlayer region. Our present work demonstrated that anion exchanging by α-$Ni(OH)_2$, containing acetate anions, was possible. Further experiments of anion exchanging by α-$Ni(OH)_2$ were conducted. Detailed results of these experiments will be reported in the future.

3. Intermediate Phase

The molar ratio of $(OCOCH_3)$/Ni in the intermediate phase is equal to half the molar ratio in the α-$Ni(OH)_2$ phase. The *d* value corresponding to basal spacing (1.415 nm) in the intermediate phase is in fair agreement with the sum (1.4375 nm) of basal spacing of α-$Ni(OH)_2$ (0.977 nm) and β-$Ni(OH)_2$ (0.4605 nm). The FT–IR spectra of the intermediate phase seemed to overlap the α- and β-$Ni(OH)_2$ spectra. This shows that the intermediate phase may contain both structures of α- and β-$Ni(OH)_2$. But the chemical reaction of the intermediate phase with *n*-propylamine and alkyl-carboxylate showed that the intermediate phase is a single phase and does not contain α- and β-$Ni(OH)_2$. Furthermore, this phase was very unstable. These results suggests that the intermediate phase may be the second stage compound (21).

The isolation of ordered intercalation compounds in which the layers are partially filled with guest ions or molecules is known as staging and is one of the most fascinating aspects of the intercalation chemistry of lamellar materials. In particular, the literature describing graphite intercalation reactions contains numerous examples of staging intermediates (22–23). However, staging in host lattices other than graphite is much less common but has been observed on

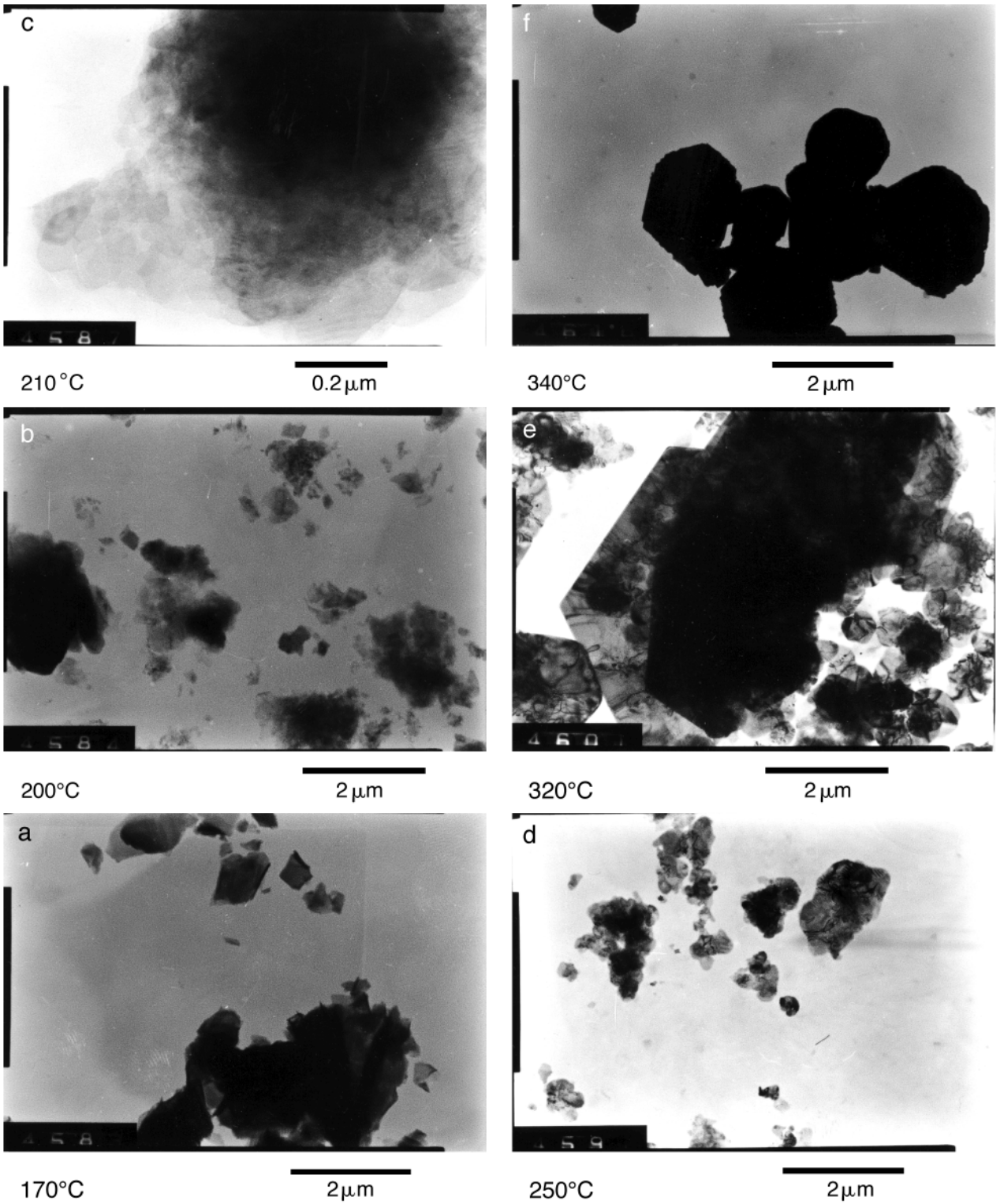

FIG. 4. TEM photographs of the samples obtained at the indicated temperatures during heating of nickel acetate solution.

a few occasions for transition metal dichalcogenides (22, 24–26). The common occurrence of this phenomenon in graphite is thought to be as a consequence of the flexible nature of the graphite with single-atom layers. Such staging should not be observed in clay with layers many atoms thick. Recently, time-resolved *in situ* energy-dispersive

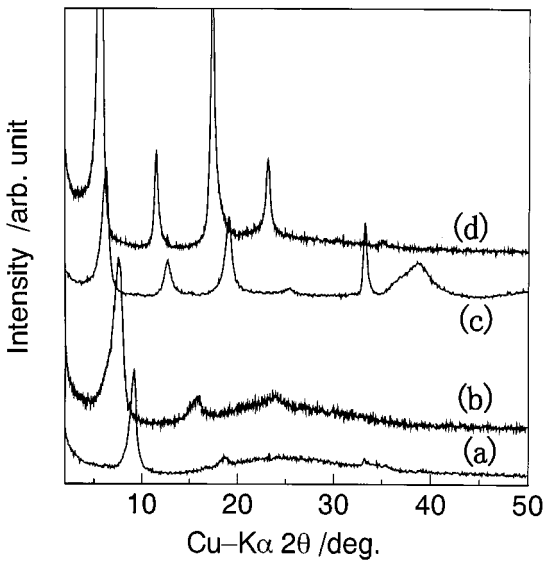

FIG. 5. XRD patterns (a) of the sample in Fig. 1a, (b) after intercalation reaction of (a) with *n*-propylamine, (c) of the sample in Fig. 1e, and (d) after intercalation reaction of (c) with *n*-propylamine.

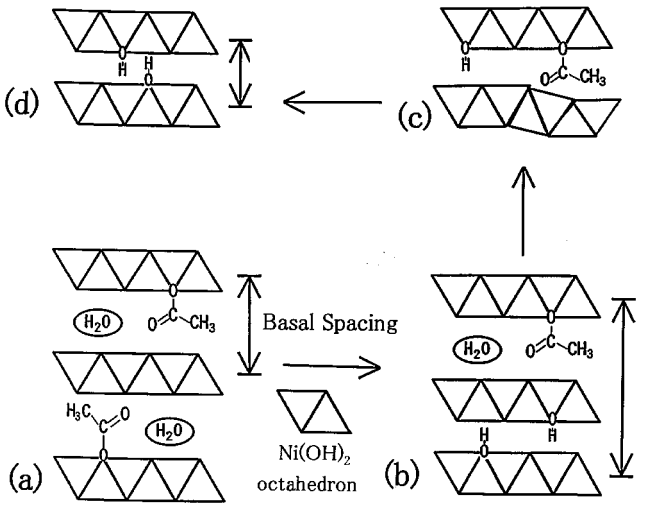

FIG. 7. Schematic diagram of the crystallization process of (a) α-$Ni(OH)_2$, (b) second-stage compound, (c) disordered β-$Ni(OH)_2$, and (d) ordered β-$Ni(OH)_2$.

X-ray diffraction studies on the intercalation of dicarboxylate anions into $[LiAl_2(OH)_6]ClH_2O$ with hydrotalcite structure have revealed the rapid formation of a second-stage intermediate phase that subsequently transforms into a pure phase fully ion-exchanged product (21). These intermediates were isolated as pure crystalline phases by reaction of the host lattice with stoichiometric amounts of the dicarboxylate anions. The staging in this system was explained by the Roedorff model (27), where every second layer contains the dicarboxylate guest, rather than by the Daumas–Herold model (28), which would require buckling of the layers. Thus the possibility of occurrence of the staging in rigid layers was first found. Our results seemed to be the case in the intermediate step of the release of guest molecules (acetate anions) from the layer structure.

Furthermore, the second-stage structure seemed to be preserved after anion exchange. If the alkyl-carboxylate ions occupy all the interlayer spacing, the interlayer distances should be equal to those of exchanged α-$Ni(OH)_2$.

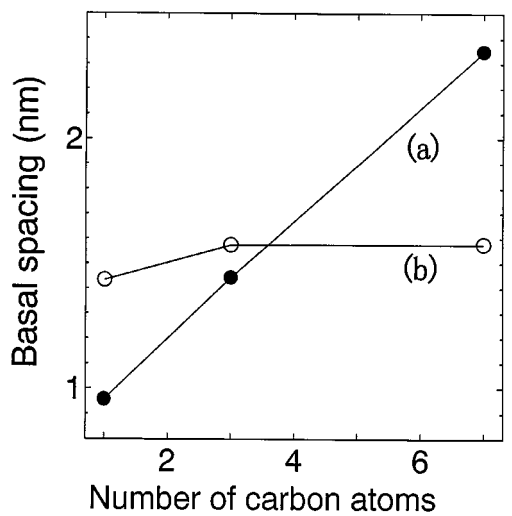

FIG. 6. Basal spacing changes by alkyl-carboxylate exchanging of (a) the sample in Fig. 1a and (b) the sample in Fig. 1e as a function of the number of carbon atoms in the alkyl chain.

CONCLUSION

$Ni_2(OH)_3(OCOCH_3)1.4H_2O$, which is a hydrotalcite-like phase and anion-exchangeable, first crystallized by constant-rate heating of nickel acetate solution. The acetate ions in the interlayer region were gradually released with increasing temperature (Fig. 7a). The second-stage compound, $Ni_2(OH)_{3.5}(OCOCH_3)_{0.5}0.5H_2O$, formed as an intermediate phase under restricted conditions (Fig. 7b). At 210°C, β-$Ni(OH)_2$ with a small amount of acetate ions and structural disordering formed (Fig. 7c). The release of acetate ions and the structural ordering occurred with increasing temperature, resulting in the formation of hexagonal-shaped β-$Ni(OH)_2$ crystals with a mean diameter of 10 μm at 320°C (Fig. 7d).

REFERENCES

1. E. Tani, M. Yoshimura, and S. Somiya, *J. Am. Ceram. Soc.* **64**(12), c-181 (1981).
2. T. Mitsuhashi, M. Ichihara, and U. Tatsuke, *J. Am. Ceram. Soc.* **57**(2), 97–101 (1974).
3. H. Nishizawa, N. Yamazaki, K. Matsuoka, and H. Mitsushio, *J. Am. Ceram. Soc.* **57**(7), 343 (1982).

4. Q. W. Chen, Y. T. Qian, H. Qian, Z. Y. Chen, W. B. Wu, and Y. H. Zhang, *Mater Res. Bull.* **30,** 443 (1995).
5. M. Yoshimura, S. E. Yoo, M. Hayashi, and N. Ishizawa, *Jpn. J. Appl. Phys.* **28,** L2007 (1989).
6. S. E. Yoo, M. Hayashi, N. Ishizawa, and M. Yoshimura, *J. Am. Ceram. Soc.* **73,** 2561 (1990).
7. H. Nishizawa and K. Yuasa, *J. Mater. Sci. Lett.* **17,** 985 (1998).
8. H. Nishizawa and K. Yuasa, *J. Solid State Chem.*, in press.
9. C. Greaves and M. A. Thomas, *Acta Crystallogr.* **B42,** 51 (1986).
10. P. Genin, A. Delahaye-Vidal, F. Portemer, K. Tekaia-Elhsissenand, and M. Figlarz, *Eur. J. Solid State Inorg. Chem.* **28,** 505 (1991).
11. H. Nishizawa, T. Tani, and K. Matsuoka, *J. Am. Ceram. Soc.* **67,** c-98 (1984).
12. H. Nishizawa, N. Yamasaki, K. Matsuoka, and Mitsushio, *J. Am. Ceram. Soc.* **65,** 343 (1982).
13. L. Guerlou-Demourgues, C. Denage, and C. Delmas, *J. Power Sources* **52,** 269 (1994).
14. C. Cabannes-Ott, *Ann. Chim.* **5,** 905 (1960).
15. M. Figlarz, J. Guenot, and S. Le Bihan, *C. R. Acad. Sci. C* **270,** 2131 (1970).
16. P. Oliva, J. Leonardi, F. Laurent, C. Delmas, J. Braconnier, M. Figlarz, F. Fievet, and A. de Guibert, *J. Power Sources* **8,** 229 (1982).
17. M. Dixit, G. N. Sibbanna, and P. V. Kamath, *J. Mater. Chem.* **6,** 1429 (1996).
18. K. Nakamoto, "Infrared and Ramman Spectra," p. 233. Wiley, New York, 1986.
19. P. Genin, A. Delahaye-Vidal, F. Portemer, K. Tekaia-Elhsissen, and M. Figlarz, *Eur. J. Solid State Inorg. Chem.* **28,** 505 (1991).
20. P. V. Kamath and G. H. A. Therese, *J. Solid State Chem.* **128,** 38 (1997).
21. A. M. Fogg, J. S. Dunn, and D. O'Hare, *Chem. Mater.* **10,** 356 (1998).
22. W. Rudorff, *Chimica* **19,** 489 (1965).
23. A. Herord, *Synth. Met.* **23,** 27 (1988).
24. M. Danot, A. L. LeBlanc, and J. Rouxel, *J. Bull. Soc. Chim. Fr.* **8,** 2670 (1969).
25. J. Rouxel, J. Cousseau, and L. Trichet, *C. R. Acad. Sci. Paris C* **273,** 243 (1971).
26. A. LeBlanc, L. Trichet, M. Danot, and J. Rouxel, *J. Mater. Res. Bull.* **9,** 191 (1974).
27. W. Roedorff, *Z. Phys. Chem.* **45,** 42 (1940).
28. N. Daumas and A. Herold, *C. R. Acad. Sci. Paris C* **268,** 373 (1969).